Atmos. Chem. Phys. Discuss., 3, 3991–4036, 2003
www.atmos-chem-phys.org/acpd/3/3991/

Atmospheric Chemistry and Physics Discussions

The isotope composition of water vapour: A powerful tool to study transport and chemistry of middle atmospheric water vapour

Ch. Bechtel[1] and A. Zahn[2]

[1]Institut für Umweltphysik, University of Heidelberg, Heidelberg, Germany
[2]Institute of Meteorology and Climate Research, Forschungszentrum Karlsruhe, Germany

Received: 11 June 2003 – Accepted: 16 July 2003 – Published: 28 July 2003

Correspondence to: A. Zahn (andreas.zahn@imk.fzk.de)

Abstract

A one-dimensional chemistry model is applied to study the stable hydrogen (D) and stable oxygen isotope (^{17}O, ^{18}O) composition of water vapour in stratosphere and mesosphere. The stable isotope ratios of tropospheric H_2O are determined by "physical" fractionation effects, i.e. phase changes, diffusion processes, and mixing of air masses. Due to these processes water vapour entering the stratosphere (i) is mass-dependently fractionated (MDF), i.e. shifts in the isotope ratio $^{17}O/^{16}O$ are ~0.52 times of those of $^{18}O/^{16}O$ and (ii) shows isotope shifts in D/H, which are ~5 times of those in $^{18}O/^{16}O$. In stratosphere and mesosphere "chemical" fractionation, that are the oxidation of methane, re-cycling of H_2O via the HO_x family, and isotope exchange reactions are shown to considerably enhance the isotope ratios in the imported tropospheric H_2O. Enrichments relative to the isotope ratios at the tropopause are used to derive the partitioning of tropospheric (unmodified), re-cycled and in situ generated H_2O. The model reasonably predicts overall increases of the stable isotope ratios in H_2O by ~23% for D/H, ~8.5% for $^{17}O/^{16}O$, and ~14% for $^{18}O/^{16}O$. The $^{17}O/^{16}O$ and $^{18}O/^{16}O$ ratios in H_2O are shown to be a measure of the partitioning of HO_x that receives its O atom either from the reservoirs O_2 or O_3. In the entire middle atmosphere, MDF O_2 is the major donator of oxygen atoms incorporated in OH and HO_2 and thus in H_2O. It is demonstrated that in the stratosphere mass-independent fractionation (MIF) in O_3 in a first step is transferred to the NO_x family and only in a second step to HO_x and H_2O. In contrast to CO_2, $O(^1D)$ only plays a minor role in this MIF transfer. The major uncertainty in our calculation arises from the many badly quantified isotope exchange reactions and kinetic isotope fractionation factors.

1. Introduction

Water vapour (H_2O) belongs to the most important trace gases in the Earth's atmosphere. It plays a key role as partner of homogeneous and heterogeneous chemical

ACPD

3, 3991–4036, 2003

reactions (Lelieveld and Crutzen, 1990, 1994) and in the short-wave and long-wave radiative budget of the atmosphere (IPCC, 2001). Its extremely complex atmospheric cycle is not understood in sufficient detail, particularly as atmospheric H_2O is present in the gaseous, fluid, and solid phase. Interest in middle atmospheric H_2O was additionally increased by observations made by Oltmans and Hofmann (1995) and after this by others (SPARC, 2000, and references therein, Rosenlof et al., 2001) who have found increasing H_2O concentrations of 30-150 nmol/mol yr^{-1} in the middle atmosphere since 1954. Not only the cause of this trend but also its consequences on the Earth's climate and the chemistry of the middle atmosphere is a matter of vital discussion (Forster and Shine, 1999, 2002; Kirk-Davidoff et al., 1999).

Mostly, H_2O concentration measurements, supported by atmospheric circulation models, are used to place constraints on the H_2O cycle in the middle atmosphere (Dessler et al., 1995; Rosenlof et al., 1997; Randel et al., 2001). A new dimension allows for the analysis of the isotopic composition of water vapour.

Abundances of stable isotopes in water vapour are usually reported as per mil deviation of the 'rare isotope' to the 'most abundant isotope' ratio, relative to the Vienna Standard Mean Ocean Water (V-SMOW) reference. For $\delta^{18}O$, e.g., this δ notation is $\delta^{18}O(H_2O) = (R_{^{18}O,\,sample}/R_{^{18}O,\,V-SMOW} - 1)\cdot 1000‰$, where $R_{^{18}O}$ denotes the isotope ratio $^{18}O/^{16}O$ of a sample or V-SMOW, respectively. $R_{D,\,V-SMOW}$ is $0.31152\cdot 10^{-3}$ (Hagemann et al., 1970; DeWit et al., 1980; Tse et al., 1980), $R_{^{17}O,\,V-SMOW}$ is $0.3799\cdot 10^{-3}$ (Li et al., 1988) , and $R_{^{18}O,\,V-SMOW}$ is $2.0052\cdot 10^{-3}$ (Baertschi, 1976). All δD, $\delta^{17}O$, and $\delta^{18}O$ values in this paper are given with respect to V-SMOW.

The major source of atmospheric water vapour is the ocean having the isotope composition of V-SMOW, i.e., $\delta^{18}O(H_2O) \approx 0‰$. Evaporation into the atmosphere leads to depletion in the rare H_2O isotopologues, due to their lower vapour pressure compared to the most abundant $H_2{}^{16}O$, the vapour pressure isotope effect (v.p.i.e.). Typically, $\delta^{18}O(H_2O)$ is $-12‰$ and $\delta D(H_2O)$ is $-85‰$ just above the ocean (Rozanski et al., 1993). Cooling during upward air movement causes cloud formation and due to

ACPD
3, 3991–4036, 2003

the v.p.i.e. preferential condensation and subsequent removal of the isotopically substituted H_2O isotopologues by precipitation. The D/H, $^{17}O/^{16}O$, and $^{18}O/^{16}O$ isotope ratios in H_2O thus decrease with altitude and reach tropopause values in the range of $\delta D(H_2O) \approx -(450\text{-}750)^{\circ}/_{\circ\circ}$, $\delta^{17}O(H_2O) \approx -(30\text{-}70)^{\circ}/_{\circ\circ}$, and $\delta^{18}O(H_2O) \approx -(60\text{-}130)^{\circ}/_{\circ\circ}$, respectively (see Sect. 2). This isotopically depleted water vapour is imported into the stratospheric overworld, almost exclusively within the tropics (Holton et al., 1995; Highwood and Hoskins, 1999). As a result of negligible cloud formation and subsequent precipitation or sedimentation, transport within the middle atmosphere virtually does not change this tropopause isotope signature.

In contrast to the troposphere, chemical reactions determine the isotope composition of H_2O in the middle atmosphere such as: (i) methane (CH_4) oxidation, the main in situ source of H_2O in the stratosphere, (ii) exchange of oxygen atoms with molecular oxygen and ozone via the HO_x and NO_x family, (iii) oxygen isotope exchange reactions e.g. between H_2O and OH (Greenblatt and Howard, 1988; Masgrau et al., 1999), and (iv) locally restricted, injection of H_2O by aircraft. All of these processes isotopically enrich the water vapour imported from the troposphere.

Using a one-dimensional (1-D) model it is shown, how these chemical reactions modify the stable isotope composition of middle atmospheric H_2O on the one hand, and vice versa, how H_2O isotope observations can be exploited to infer constraints on these reactions. Three previous model studies on the isotopic composition of stratospheric H_2O have been made. Kaye (1990) studied $\delta^{18}O(H_2O)$ in the middle atmosphere and suggested a remarkable increase in the $\delta^{18}O(H_2O)$ mixing ratio with altitude due to ^{18}O-rich excess water from the CH_4 oxidation. Ridal et al. (2001) and Ridal (2002) focused on $\delta D(H_2O)$ in the stratosphere. They found a strong vertical increase of $\delta D(H_2O)$, also due to CH_4 oxidation which is additionally modulated by the seasonally varying H_2O input from the troposphere ("tape recorder effect").

Here, all three stable isotopologues $\delta D(H_2O)$, $\delta^{17}O(H_2O)$, and $\delta^{18}O(H_2O)$ both in the stratosphere as well as in the mesosphere are dealt with. Special emphasis is put on the pathways of D, ^{17}O, and ^{18}O from their reservoirs CH_4, H_2, O_2, and O_3 into the

end product H_2O.

2. Available stable isotope fata of H_2O

In view of the difficulties of the measurement techniques listed below, only a few H_2O isotope observations have been conducted so far:

(i) Remote-sensing observations by infrared spectroscopy techniques (Abbas et al., 1987; Carli and Park, 1988; Guo et al., 1989; Dinelli et al., 1991, 1997; Rinsland et al., 1984, 1991; Stowasser et al., 1999; Johnson et al., 2001; Kuang et al., 2003). They reveal strong depletions of $\delta D(H_2O)$ with respect to V-SMOW which significantly decrease with altitude, from an average of $-(660 \pm 80)$‰ at the low-latitude tropopause (Moyer et al., 1996; Johnson et al., 2001) to typically $-(450 \pm 70)$‰ at 40 km. Observations by Stowasser et al. (1999) indicate extreme $\delta D(H_2O)$ depletions as low as –830‰ at 17 km inside the Arctic vortex, which was attributed to condensation and subsequent sedimentation of polar stratospheric cloud (PSC) particles.

For $\delta^{17}O(H_2O)$ and $\delta^{18}O(H_2O)$, most observations indicate values of about 0 to –100‰ and a weak, but insignificant vertical increase. This insignificance can primarily be assigned to the large measurement uncertainties of 50-120‰. Deviations from this behavior were noticed during early observations by Guo et al. (1989) who retrieved increasing $\delta^{18}O(H_2O)$ values from (80 ± 140)‰ at 22 km altitude to (400 ± 250)‰ at 37 km. Using a balloon-borne spectrometer, Johnson et al. (2001) obtained low isotope ratios of –(300-30)‰ (on the average, –128‰) for $\delta^{18}O(H_2O)$, and of –(400-0)‰ (on the average, –84‰) for $\delta^{17}O(H_2O)$ at 12-20 km altitude.

(ii) Cryogenic in situ sampling and subsequent laboratory-based mass spectrometry (MS) analysis. Apart from observations in the upper troposphere and tropopause region by Ehhalt (1974), Smith (1992), Zahn et al. (1998), and Zahn (2001), there is only one set of balloon-borne stratospheric $\delta D(H_2O)$ profiles (Pollock et al., 1980). They show a continuous increase in $\delta D(H_2O)$ with altitude, from about –450‰ at 25 km to about –360‰ at 35 km. The O isotope composition of stratospheric H_2O has not yet

been measured by this technique, which is mainly due to the small sample amounts available and their difficult handling and MS analysis.

(iii) In situ measurements by tunable diode laser absorption spectroscopy (TDLAS). This new and challenging technique was recently presented by C. Webster (2003). He reported measurement uncertainties of 30-50‰ for all stable isotope ratios D/H, $^{17}O/^{16}O$, and $^{18}O/^{16}O$ in H_2O in the UTLS region using the ALIAS instrument onboard the NASA WB57 aircraft.

3. Information provided by the H_2O isotopic composition

The isotopic composition of tropospheric water vapour is controlled by the hydrological cycle. Hence, H_2O isotope data can be used as tracers for the condensation history of probed air masses (Taylor, 1984), as applied for studying the transport of tropospheric H_2O into the lowermost stratosphere (Zahn, 2001).

Both, $\delta D(H_2O)$ and $\delta^{18}O(H_2O)$ are primarily controlled by the v.p.i.e. and thus undergo similar variations. Indeed, in surface precipitation both isotopologues are related closely by the meteoric water line (MWL): $\delta D(H_2O) \approx m \times \delta^{18}O(H_2O) + 10‰$, with $m = 8$ (Craig, 1961). This relationship was found to be valid even on Mount Logan (Canada) at 5951 m altitude, with $m = 7.5$ (Holdsworth et al., 1991). At cold temperatures as encountered in the tropical tropopause layer (TTL), however, kinetically limited isotope fractionation during formation of ice cloud particles, their lofting in convective cells and mixing of air masses showing different H_2O isotope compositions are assumed to considerably reduce $\delta D(H_2O)$ depletion compared to $\delta^{18}O(H_2O)$ (Moyer et al., 1996; Keith, 2000; Johnson et al., 2001; Kuang et al., 2003). In fact, using the isotope composition of water vapour entering the stratosphere of $\delta D(H_2O) = -679‰$ and $\delta^{18}O(H_2O) = -128‰$ measured by Johnson et al. (2001), a slope m of 5.4 is calculated. Finally and importantly, $\delta^{17}O(H_2O)$ will provide exactly the same information as $\delta^{18}O(H_2O)$, due to lack of major mass-independent isotope fractionation (MIF) in

the troposphere, that is $\Delta^{17}O(H_2O) = \delta^{17}O(H_2O) - 0.52\ \delta^{18}O(H_2O)$ will be 0‰ at the tropical tropopause.

In conclusion, it can be presumed that tropospheric water vapour entering the stratosphere at the tropical tropopause exhibits a $\delta D(H_2O)/\delta^{18}O(H_2O)$ ratio of 5-6 and is mass-dependently fractionated (MDF).

Chemical reactions in the middle atmosphere will strongly modify this isotope signature imported from the troposphere, as will be pointed out briefly below and explained in more detail later:

(i) Methane is oxidized in the middle atmosphere by reactions with OH, Cl, and $O(^1D)$, and by photolysis (Lary and Toumi, 1997). Each oxidized CH_4 molecule leads to the net formation of almost two H_2O molecules (Evans et al., 1999; Zöger et al., 1999; Michelsen et al., 2000). The δD value of the new H_2O molecule, i.e. $\delta D(H_2O)$, differs from $\delta D(CH_4)$, because the CH_4 loss reactions are accompanied by an unusually strong kinetic isotope fractionation. For instance, at room temperature the D isotope fractionation factor KIE^D, that is the ratio of the rate constants $k(CH_4)/k(CH_3D)$, is $KIE^D(OH) = 1.29$ for the reaction of CH_4 with OH, $KIE^D(Cl) = 1.51$ for the reaction with Cl, and $KIE^D(O(^1D) = 1.11$ for the reaction with with $O(^1D)$ (Saueressig et al., 1996, 2001; Tyler et al., 2000). Since these KIEs differ considerably, the $\delta D(H_2O)$ distribution in the middle atmosphere is expected to mirror the partitioning of the different CH_4 oxidation reactions. This information cannot be inferred from simultaneous CH_4 and H_2O concentration measurements.

(ii) Re-cycling of oxygen atoms between H_2O and the oxygen reservoir gases O_2 and O_3 via HO_x and NO_x species and oxygen isotope exchange reactions. Besides net H_2O formation due to CH_4 oxidation, continuous loss of H_2O and reformation of H_2O lead to an extensive turnover of oxygen atoms between oxygen containing trace gases. This process recycles ~4 times more H_2O molecules than the net production by oxidation of CH_4 (see Fig. 4). Though a zero-cycle with respect to the H_2O mass, it strongly influences the oxygen isotope composition of H_2O, i.e. in the same manner as addressed in item (i). Therefore, the MIF oxygen isotope signal transferred to middle

stratospheric H_2O is strongly amplified compared to the MIF signal originating from CH_4 oxidation alone.

A crucial and exciting point is that more than 99% of all oxygen atoms taken to form H_2O in the middle atmosphere stem from the hydroxyl radical OH. Hence, $\delta^{17}O(H_2O)$ and $\delta^{18}O(H_2O)$ data also provide information on the oxygen isotope composition of OH, and by considering $\Delta^{17}O(H_2O)$ on the affection of MIF enriched O_3 to OH_x and via OH_x to many other oxygen containing trace gases in the middle atmosphere. This MIF transfer from O_3 to oxygen-containing radicals was studied by Lyons (2001).

4. Model description

The 1-D model encompasses 64 boxes from 16 to 80 km, each 1 km high. Temperature and pressure profiles are set according to the U.S. Standard Atmosphere (1976). Vertical transport is parameterised by eddy diffusion coefficients K_z, below 29 km using the "National Academy of Science (1976)" profile , from 29 km to 50 km using the "Hunten" profile, both depicted by Massie and Hunten (1981), and above 50 km employing the profile given by Froidevaux and Yung (1982).

4.1. Peculiarities in modelling isotope ratios

The concept of chemical families frequently applied in atmospheric chemistry models mostly fails if isotopologues are considered. For instance, the reaction chain of CO + OH $\rightarrow$ CO_2 + H followed by H + O_2 + M $\rightarrow$ HO_2 + M converts OH in HO_2, which conserves the sum of HO_x = OH + HO_2. The oxygen atom of the initial OH, however, is incorporated in CO_2 and thus leaves the HO_x family. A new OH bond is formed, which has the oxygen isotope composition of O_2.

Isotope exchange reactions such as the fast O exchange between O_2 and $O(^3P)$ (Kaye and Strobel, 1983) also have to be considered. They modify isotope ratios but not the concentration of the participating species.

ACPD
3, 3991–4036, 2003

Finally, when including isotopologues that contain two or more of the isotopes of interest such as O_3 or HO_2, the individual isotopologues have to be considered separately, e.g. the OQO and OOQ or HQO and HOQ (with Q the rare isotope).

4.2. Trace gas chemistry

Due to negligible cloud formation in the middle atmosphere, our model is restricted to gas phase chemistry. Initially, all reactions involved in significant H_2O chemistry and isotope exchange with other gases were assessed carefully for all altitudes considered by the model. The reactions finally used (Tables 1 and 2) always account for more than 95% of the local chemical turnover of H_2O and its isotopes at a given altitude.

Water vapour is formed due to H-abstraction by OH, i.e. $XH_i + OH \rightarrow XH_{i-1} + H_2O$, where XH_i is CH_4 (reaction R1), CH_2O (R7), HO_2 (R15), HCl (R20), H_2 (R25), or HNO_3 (R28). The major sinks of middle atmospheric H_2O are the reaction with $O(^1D)$ (R29) and photolysis at wavelength below 200 nm (R30).

Furthermore, all reactions that are necessary to maintain the overall budget of O- and H-atoms balanced are included. To this end a complete methane destruction scheme (LeTexier et al., 1988) is applied which is initialised by photolysis and the reaction of CH_4 with OH, $O(^1D)$, Cl. All relevant reactions of the OH_x-family (Burnett and Burnett, 1995) are also considered.

The concentrations and the isotopic compositions of H_2O, OH, HO_2, H, H_2, CH_4, CH_3, CH_2O, HCO, HNO_3, and HCl are explicitly calculated by the model.

4.3. Isotope chemistry

Integration of isotopologues renders the model complex, as shown for the initial steps of the major methane destruction reactions (Table 3).

Only for a few of the reactions listed in Table 1 is the isotope fractionation factor KIE $= k/k'$ known, with k the rate constant and the slash marks the isotopically substituted species. All KIEs that have been measured in the laboratory are implemented in the

ACPD
3, 3991–4036, 2003

model.

For all other reactions KIE is set to $(\mu'/\mu)^{1/2}$, with μ the reduced mass of the reactants. This accounts for the fact that the rate constant of a certain reaction does not only depend on the reactivity of the reactants, but also on their collision frequency.

Additionally, the oxygen exchange reactions listed in Table 4 were included, partially for deriving the necessary isotope parameter profiles.

4.4. Trace gas parameter profiles

Fixed, globally, seasonally and diurnally averaged profiles are used for the following trace gases: O_3, $O(^1D)$, NO, NO_2, and Cl as retrieved by the 2-D model version of ECHAM 3 (C. Brühl, Max-Planck-Institute for Chemistry, Mainz), a mean $O(^3P)$ profile measured by CHRISTA onboard the Space Shuttle in November 1994 (with the courtesy of M. Kaufmann, University of Wuppertal), and CO measured by ISAMS onboard the UARS satellite (López-Valverde et al., 1996).

4.5. Isotope parameter profiles of $O(^3P)$, O_3, $O(^1D)$, and NO

The oxygen isotope compositions assumed for O_2, $O(^3P)$, O_3, and $O(^1D)$ are indicated in Fig. 1 together with the calculated profiles for NO, OH, and HO_2.

The isotope composition of $O(^3P)$ is set to the one of O_2, i.e., $\delta^{17}O(O_2) = 11.8‰$ and $\delta^{18}O(O_2) = 23.8‰$ (Luz et al., 1999; Coplen et al., 2002), because of the rapid O exchange between $O(^3P)$ and O_2 (Kaye and Strobel, 1983).

The isotope composition of O_3 was set to be solely dependent on temperature, as it was found recently that all reliable atmospheric data apparently agree with the enrichments determined in laboratory studies (Mauersbeger et al., 2001) and that pressure dependence is negligible below 100 hPa. The (consistent) laboratory data by Thiemens and Jackson (1988, 1990), Morton et al. (1990), and (Günther et al., 1999) are implemented under the assumption that 80% of the isotope enrichment of O_3 is carried by

the asymmetric QOO (Anderson et al., 1989; Janssen et al., 1999; Mauersberger et al., 1999).

$Q(^1D)$ is derived from the isotope enrichment in O_3 under the following assumptions: (i) 80% of the isotope enrichment in O_3 is located in the asymmetric OOQ, (ii) during the photolysis of O_3 only the outer oxygen atoms form $O(^1D)$, (iii) there is negligible fractionation during the photolysis of O_3 (Wen and Thiemens, 1993), and (iv) mass-dependent collision rates during subsequent quenching of $O(^1D)$ on N_2 and O_2 to the ground state $O(^3P)$ lead to an additional isotope enrichment of 19‰ for $\delta^{17}O$ and 36‰ for $\delta^{18}O$ in $O(^1D)$ (calculated by using the formula given in Sect. 4.3).

The oxygen isotope composition of middle atmospheric NO_x is not controlled by its main source, i.e. oxidation of N_2O by $O(^1D)$, but by O exchange between O_x and NO_x:

$$NO + O_3 \rightarrow NO_2 + O_2 \qquad \text{(NO-1)}$$

$$NO_2 + O(^3P) \rightarrow NO + O_2 \qquad \text{(NO-2)}$$

and the fast O - exchange reactions:

$$NO + Q(^3P) \leftrightarrow NQ + O(^3P) \qquad \text{(NO-3)}$$

$$NO + QH \leftrightarrow NQ + OH \qquad \text{(NO-4)}$$

Indeed, over the entire altitude range considered less than 0.5% of all O atoms in NO stem from the oxidation of N_2O by $O(^1D)$. Hence, the isotopic composition of N_2O that is known to carry MIF into the stratosphere (Cliff and Thiemens, 1997; Cliff et al., 1999; Röckmann et al., 2001; Kaiser et al., 2002) does not have to be considered. The O isotope ($\delta^{17}O$, $\delta^{18}O$) parameter profile of NO is derived by calculating the source partitioning of the reactions NO-1 to NO-4. The inferred enrichments exceed the ones calculated by Lyons (2001) by almost a factor of two, as outlined in Sect. 6.4. Because of the dominance of NO-3, the oxygen isotopic composition of NO in the mesosphere is very similar to the one of $O(^3P)$.

4.6. Boundary conditions

At the lower model boundary, i.e., the tropopause (16 km), fixed trace gas and isotope mixing ratios are set as follows: $[H_2O] = 3.48\,\mu$mol/mol. $\delta D(H_2O) = -660‰$ and $\delta^{18}O(H_2O) = -128‰$ (Moyer et al., 1996; Johnson et al., 2001). $\Delta^{17}O(H_2O)$ is set to 0‰ (as no process is known in the troposphere, which could cause MIF in H_2O), so that $\delta^{17}O(H_2O)$ is –66‰ (this value agrees with –(84 ± 31)‰ observed by Johnson et al. (2001)). $[CH_4] = 1.7\,\mu$mol/mol. $\delta D(CH_4) = -86‰$ (Quay et al., 1999). $[H_2] = 0.55\,\mu$mol/mol (Zöger et al., 1999). $\delta D(H_2) = 120‰$ (Friedman and Scholz, 1974). The flux of all considered species across the upper boundary (80 km) is set to zero.

5. Model results and comparison with observations

5.1. Vertical profile of $\delta D(H_2O)$

The calculated $\delta D(H_2O)$ profile compares well with observations and the model results obtained by Ridal (2002) (Fig. 2). Apart from the Arctic profile retrieved by (Stowasser et al., 1999), the available observations (Sect. 2) show a vertical increase by ~(150-200)‰ between 20 and 40 km, but partially differ in absolute concentration. Consider however the large measurement uncertainty of all infrared instruments of ±(60-150)‰. The $\delta D(H_2O)$ profiles obtained by balloon-borne in situ H_2O sampling and subsequent laboratory analysis by Pollock et al. (1980) (reported uncertainties: ~50‰) reveal significantly higher values compared to the other measurements and the model.

As mentioned in Sect. 3, the strong vertical $\delta D(H_2O)$ increase in the stratosphere is due to the increasing fraction of H_2O that originates from the oxidation of CH_4. The $\delta D(H_2O)$ value in the mesosphere, which is higher than the tropopause value by ~250‰, indicate that ~60% of the mesospheric H_2O originate from the troposphere and ~40% stem from the oxidation of CH_4 (see Sect. 6.2).

5.2. Vertical Profiles of $\delta^{17}O(H_2O)$ and $\delta^{18}O(H_2O)$

The O isotope ratios in H_2O (Fig. 3) exhibit a vertical profile that is similar to that of $\delta D(H_2O)$. The reason is oxygen exchange between O_2 and O_3 via HO_x- and NO_x-species rather than the net formation of H_2O as a final product of CH_4 oxidation than (see Sect. 6.3).

The measurements by Dinelli et al. (1991), Guo et al. (1989), Rinsland et al. (1991), and Johnson et al. (2001) are in reasonable agreement with our model results. However the large measurement errors of ±(50-120)‰ have to be noted, which compares with the calculated total vertical increase by 85‰ for $\delta^{17}O(H_2O)$ and 140‰ for $\delta^{18}O(H_2O)$.

6. Discussion

6.1. The middle atmospheric water vapour budget

Figure 4 shows the inferred budgets of H_2O, $\delta D(H_2O)$ and $\delta^{18}O(H_2O)$ of the middle atmosphere. The annual flux of tropospheric water into the stratosphere is set to 788 Mt as given by (Yang and Tung, 1996). In the stratosphere further net production of 50.3 Mt of H_2O (and of 0.4 Mt of H_2) takes place due to the oxidation of CH_4 with a calculated net CH_4 destruction rate of 24 Mt yr^{-1}. This is slightly lower than the (40 ± 10) Mt yr^{-1} mostly reported (Crutzen, 1995; Lelieveld et al., 1998), but agrees with Gettelmann et al. (1998) and exceeds earlier values given by Crutzen (1991) and Khalil et al. (1993). The calculated ratios between H_2O and H_2 production and CH_4 loss for the entire middle atmosphere are:

$$\frac{P(H_2O)}{L(CH_4)} = 1.87 \quad \text{and} \quad \frac{P(H_2)}{L(CH_4)} = 0.13 \tag{1}$$

Using a coupled chemistry/dynamical model (LeTexier et al., 1988) derived $P(H_2O)/L(CH_4) = 1.6$ which is in agreement with satellite observations by Hanson and Robinson (1989). More recent in situ measurements indicated higher values of 1.94 ± 0.27 (Dessler et al., 1994), 1.82 ± 0.21 (Engel et al., 1996), 1.973 ± 0.003 (Hurst et al., 1999), and 1.975 ± 0.030 (Zöger et al., 1999), which are in reasonable agreement with our model results.

Interestingly, although each CH_4 molecule finally results in the formation of almost 2 H_2O molecules (Eq. 1), most hydrogen atoms in CH_4 make the detour via H_2, the HO_x family, and other gases to H_2O, as demonstrated in Fig. 5. Only ~15% of all H_2O molecules are formed directly from one of the four H atoms of CH_4 or intermediate products in the CH_4 destruction chain (such as formaldehyde, CH_2O), i.e., they are produced via the following reactions:

$$CH_4 + OH \rightarrow CH_3 + H_2O \tag{R1}$$

$$CH_2O + OH \rightarrow HCO + H_2O \tag{R7}$$

This can be explained by the fact that only ~30% of all CH_4 molecules react with OH, and the majority of ~70% with $O(^1D)$ or Cl (Lary and Toumi, 1997), which is in strong contrast to the troposphere where the reaction with OH clearly dominates. The other ~85% of the H atoms in CH_4 are incorporated first in the HO_x family (~60%), in H_2 (~18%), and other gases such as HCl (~7%), before they end up in H_2O. This detour of the H atoms from CH_4 to H_2O certainly affects not only the isotope composition of the final product H_2O, but also that of the intermediate products (OH, HO_2, HCO, H, H_2, HCl etc.).

Figure 6 presents the vertical profile of H_2O production $P(H_2O)$ and loss $L(H_2O)$. Both $P(H_2O)$ (dominated by the reaction $OH + HO_2 \rightarrow H_2O + O_2$ (Kaye, 1990)) and $L(H_2O)$ (more than 99% of which are due to the reaction of $H_2O + O(^1D) \rightarrow 2\,OH$) peak at ~38 km altitude. The net rate, $P(H_2O) - L(H_2O)$, amounts to ~25% of $P(H_2O)$ only. It shows a wide maximum centred at 35-40 km, that is ~5 km above the maximum of the

CH_4 loss rate (for better comparison 2 × L(CH_4) is shown, dotted line). This again emphasises that (i) most H atoms from CH_4 are first incorporated in intermediate species (that experience spatial redistribution) before ending up in H_2O, and (ii) a considerable turnover of H_2O molecules occurs in the middle atmosphere which significantly exceeds the net production of H_2O.

Division of the local H_2O concentration by the local H_2O loss rate L(H_2O) yields the chemical lifetime of H_2O, $\tau(H_2O)$, at a certain altitude (Fig. 6b). In the entire middle atmosphere $\tau(H_2O)$ considerably exceeds the vertical transport time scale, i.e. H_2O never is in photochemical equilibrium. Only between 30 and 50 km altitude, the transport lifetime H^2/K_z (H being the local scale height and K_z the vertical eddy diffusion coefficient) almost compare with the photochemical lifetime of H_2O, in agreement with (LeTexier et al., 1988).

This long chemical lifetime of H_2O implies that below 30-35 km (where $\tau(H_2O)$ exceeds ~5 years) the D/H isotope ratio of H_2O is simply due to the mixing of the $\delta D(H_2O)$ isotope signature imported from the troposphere and the one present in the upper stratosphere. This finding does not apply to $\delta^{17}O(H_2O)$ and $\delta^{18}O(H_2O)$, because of the considerable oxygen exchange of H_2O with other gases, which also occurs in the lower stratosphere.

6.2. $\delta D(H_2O)$ as tracer for CH_4 oxidation

Tropospheric H_2O is imported into the stratosphere with $\delta D(H_2O) \approx -660‰$ (Moyer et al., 1996, Johnson et al., 2001). Tropospheric CH_4 carries much higher δD values of roughly –86‰ (Quay et al., 1999) into the stratosphere. Neglecting the small net formation of H_2 due to CH_4 oxidation (~0.4 Mt yr^{-1}, see Fig. 4a), a simple mass balance

for δD yields an average $\delta D(H_2O)$ value in the middle atmosphere δD_0 of:

$$\underbrace{\delta D_0 \overbrace{M_0}^{838}}_{\text{mean}} = \underbrace{\overbrace{\delta D_t}^{-660‰} \overbrace{M_t}^{788}}_{\text{import from troposphere}} + \underbrace{\overbrace{\delta D_m}^{-86‰} \overbrace{M_m}^{50}}_{\text{production from } CH_4 \text{ oxidation}} \quad (2)$$

where M_i denotes the H_2O mass fluxes of the different components and δD_i their D isotope signature. The numbers are given in per mil for δD_i and in Mt yr^{-1} for M_i, as shown in Fig. 4a and b. Equation (2) gives an average middle atmospheric $\delta D(H_2O)$ value of $\delta D_0 = -626‰$, which exceeds the value at the tropopause by 34‰ only. This small isotope excess reflects the fact that net H_2O production from CH_4 oxidation (~50 Mt yr^{-1}) is small compared to the H_2O inflow from the troposphere (~788 Mt yr^{-1}).

The vertically increasing contribution of H_2O produced by the oxidation of CH_4 is described by the upper x axis of Fig. 2. It shows the local fraction of H_2O from CH_4 oxidation $\mathcal{F}$, that is the ratio between the difference of the local $\delta D(H_2O)$ value to the tropopause value (–660‰) and the difference of the $\delta D(H_2O)$ from the CH_4 oxidation (set to –86‰) and the $\delta D(H_2O)$ tropopause value, i.e., $\mathcal{F} = (\delta D(H_2O) - (-660‰)) / (-86‰ - (-660‰))$. Figure 2 indicates that ~40% of the H_2O above 40 km originate from the oxidation of CH_4.

It might be argued that this estimation is not correct, since the high kinetic isotope fraction factors KIEs of the CH_4 oxidation reactions (Sect. 3) result in a strong vertical change of the δD value of freshly produced H_2O. Although this comment is correct, influence on $\delta D(H_2O)$ is weak, as demonstrated by Fig. 7. Because of the large KIEs, $\delta D(CH_4)$ increases from –86‰ at the tropopause to about +190‰ at the stratopause. Over the same altitude range, $\delta D(H_2O)$ rises from –660‰ to –445‰, but only by 20‰ more to –425‰ if isotope fractionation is not considered (KIEs = 1). This small difference is due to the fact that around 38 km, where the major destruction of CH_4 occurs (Fig. 6), $\delta D(CH_4)$ is about +70‰ vs. VSMOW (or 1.070 absolute) and the mean KIE is ~1.2 only (as there ~60% of all CH_4 molecules are removed by the reaction with

ACPD
3, 3991–4036, 2003

$O(^1D)$ which is associated with weak isotope fractionation). Therefore, the H_2O produced at 38 km shows a mean δD value of 1.070 / 1.2 = 0.892 absolute or –108‰ vs. VSMOW. This value does not differ much from $\delta D(CH_4)$ = –86‰ and indeed demonstrates that the high KIEs of the CH_4 loss reactions cause a weak shift in $\delta D(H_2O)$ only. Unfortunately, this finding also documents that the $\delta D(H_2O)$ value does not constitute a sensitive tracer to distinguish between the different CH_4 loss reaction chains, contrary to its initial assumption. Such a distinction could only be made with the aid of precise mass-spectrometry measurements on middle atmospheric H_2O samples (which are not available to date).

Another surprising feature is that both, the δD value of the source molecule CH_4 and the one of the end product H_2O increase with altitude (Fig. 7), although mass conservation for δD suggests the opposite behaviour, at a first glance. In all methane oxidation reactions the most abundant CH_4 reacts faster than the isotopically substituted CH_3D (Sect. 3). Therefore, the remaining CH_4 is continuously enriched in D/H with altitude (solid line in Fig. 7), while that of the freshly formed H_2O molecule is always significantly lower (dotted line) compared to the remaining CH_4. Despite this D depletion with respect to $\delta D(CH_4)$, freshly formed H_2O still shows much higher δD values than the H_2O lofted from below.

6.3. $\delta^{17}O(H_2O)$ and $\delta^{18}O(H_2O)$ as tracer for transport and chemistry

As outlined in Sect. 3, the oxygen isotope signature atom of middle atmospheric water vapour is determined by the partitioning of four oxygen isotope sources: (1) mass-dependently fractionated (MDF) H_2O imported from the troposphere, (2) mass-independently fractionated (MIF) H_2O formed as a final product of the oxidation of CH_4, (3) likewise MIF carrying H_2O from the recycling of H_2O via the HO_x family and (4) oxygen atom exchange between H_2O and other gases.

The $\delta^{17}O$ and $\delta^{18}O$ values of source (1), i.e. of H_2O imported from the troposphere, are about –67‰ and –128‰, respectively (see Sect. 4.6). The δO values of the iso-

tope sources (2) to (4), i.e. of the chemical reactions leading to new H_2O molecules, are adopted from the respective educt molecules. As outlined by Kaye (1990) and confirmed by our calculations, more than 99% of all H_2O molecules generated in the middle atmosphere are due to hydrogen abstraction from H-containing molecules by OH. Thus, the isotope sources (2) and (3) will show the O isotope signature of OH at the respective altitude. H_2O undergoes oxygen isotope exchange (i.e. isotope source 4) with OH and NO_2 (Table 4). Both oxygen exchange reactions are too slow to significantly affect the isotope composition of H_2O in the middle atmosphere.

Therefore, modifications of the oxygen isotope composition of middle atmospheric H_2O are almost exclusively controlled by reactions with OH. For this reason, the sources of OH and their oxygen isotope signatures will be studied next. As the reaction chains, by means of which OH is converted into HO_2 and back into OH without breaking the initial OH bond, form a zero cycle with respect to the oxygen isotopic composition, only the reactions forming new OH bonds need to be considered.

6.3.1. The formation of new OH bonds

Four classes of reactions, distinguished by the O isotope signal transferred, form new OH_x bonds:

(i) HO_x that receives the oxygen isotope signature from molecular oxygen via

$$CH_3O + O_2 \rightarrow HO_2 + CH_2O \quad \text{(R5)}$$

$$HCO + O_2 \rightarrow HO_2 + CO \quad \text{(R11)}$$

$$H + O_2 + M \rightarrow HO_2 + M \quad \text{(R12)}$$

Reactions R5 and R11 are part of the CH_4 oxidation chain and only play a role below 40 km. Reaction R12 dominates the formation of new OH bonds over the entire middle atmosphere. In addition, oxygen isotope exchange between OH_x and O_2 may occur via:

$$HQ + O_2 \leftrightarrow OH + OQ \quad \text{(R34)}$$

$$HOQ + O_2 \leftrightarrow HO_2 + OQ \quad \text{(R35)}$$

Assuming the rate constants of reactions R34 and R35 at their estimated upper limit, this oxygen isotope exchange with the O_2 reservoir will remarkably influence the isotope composition of OH_x and thus of H_2O, as shown by Lyons (2001) and verified here (Fig. 3).

(ii) HO_x that receives the oxygen isotope signature from MIF carrying ozone via

$$H + O_3 \rightarrow OH + O_2 \quad \text{(R13)}$$

which is important above 40 km only. Although O_3 also influences the isotope composition of HO_2 via $OH + O_3 \rightarrow HO_2 + O_2$, new OH bonds are not formed. The reason is that the oxygen atom OH receives from O_3 is lost again, simply because HO_2 is an asymmetric molecule (H–O–O).

(iii) HO_x that receives the oxygen signature from MIF carrying $O(^1D)$ and, in the case of reaction R29, from H_2O:

$$CH_4 + O(^1D) \rightarrow OH + CH_3 \quad \text{(R2)}$$

$$H_2 + O(^1D) \rightarrow OH + H \quad \text{(R26)}$$

$$H_2O + O(^1D)2\,OH \quad \text{(R29)}$$

with reaction R29 clearly dominating in the entire middle atmosphere.

(iv) HO_x that receives the oxygen isotope signature from NO_x:

$$QH + NO \leftrightarrow OH + NQ \quad \text{(R31)}$$

$$QH + NO_2 \leftrightarrow OH + NOQ \quad \text{(R32)}$$

while the oxygen isotope composition of NO_x is controlled by reactions with the O_2 and O_3 reservoirs (Sect. 4.4).

6.3.2. The origin of oxygen atoms incorporated in H_2O

On the basis of Sect. 6.3.1, the influence of each oxygen emission source (O_2, O_3, $O(^1D)$, and NO_x) on the oxygen isotope composition of freshly produced H_2O is assessed. As demonstrated in Fig. 8 and listed in Table 5, molecular oxygen clearly dominates as source of oxygen atoms transferred to water vapour in the entire middle atmosphere. When neglecting the additional not yet quantified oxygen exchange with O_2 (reactions R34 and R35, Sect. 6.3.1), of all oxygen isotopes incorporated in H_2O in stratosphere and mesosphere, respectively, ~78% and ~70% stem from O_2, ~17% and ~30% from O_3, ~2% and ~0% from $O(^1D)$, and ~2% and ~0% from other gases such as HNO_3 or H_2O itself. When assuming the additional oxygen exchange reactions R34 and R35 at their estimated upper limit, the oxygen isotope source partitioning will hardly change in the mesosphere. On the contrary, in the stratosphere the hydroxyl radical and thus the water molecules freshly produced will almost completely adopt the oxygen isotopic composition of O_2. In this case, no mass-independent fractionation is transferred to H_2O. Another finding is that in the stratosphere ~50% of the overall oxygen isotope transfer to H_2O proceed in two steps (Fig. 8), i.e. from O_2 and O_3 to NO_x and from there via HO_x to H_2O.

The oxygen isotope source partitioning just described is reflected by the strongly structured vertical profiles of $\delta^{17}O(H_2O)$ and $\delta^{18}O(H_2O)$ of freshly produced H_2O (Fig. 9). Two maxima occur, both by oxygen atom transfer from O_3 to H_2O. In the stratosphere, it is due to the oxygen transfer chain $O_3 \xrightarrow{O} NO_x \xrightarrow{O} HO_x \xrightarrow{O} H_2O$. In the mesosphere, it is caused by $H + O_3 \rightarrow OH + O_2$ (reaction R13) and subsequent O transfer from OH to H_2O due to the strongly increasing concentrations of atomic hydrogen. If the oxygen exchange reactions R34 and R35 are additionally considered, freshly produced H_2O in the stratosphere will have the $\delta^{17}O(H_2O)$ and $\delta^{18}O(H_2O)$ values of O_2.

6.3.3. $\Delta^{17}O(H_2O)$ as a tracer of MIF transfer from O_3 to H_2O

The last Sect. 6.3.2 revealed that the pathway of MIF from O_3 to H_2O is different compared to the one from O_3 to CO_2. CO_2 is assumed to receive the MIF signal exclusively from $O(^1D)$ (produced by the photolysis of O_3) via the short-lived intermediate CO_3' (Yung et al., 1991, 1997; Barth and Zahn, 1997). In the case of H_2O, $O(^1D)$ is only weakly involved in the oxygen isotope transfer (Table 5). In the stratosphere water vapour receives only ~15% of its MIF signal from $O(^1D)$. In the mesosphere $O(^1D)$ does not play any role at all.

As indicated in Fig. 8, in the stratosphere MIF transfer from O_3 to H_2O basically proceeds in three steps, first MIF transfer from O_3 to NO_x species (via reaction NO-1: $NO + O_3 \longrightarrow NO_2 + O_2$, Sect. 4.5), then from NO_x to OH_x and finally transfer to H_2O due to H-abstraction by OH. This quite efficient oxygen transfer chain leads to peaking $\Delta^{17}O(H_2O)$ values of ~10‰ at ~35 km altitude (Fig. 10). In the mesosphere, NO_x species are not involved. There, the entire MIF transfer from O_3 to HO_x (and from there to H_2O) proceeds via reaction R13: $H + O_3 \longrightarrow OH + O_2$.

6.4. Assessment Of results

A simple 1-D box model that considers relatively few chemical reactions was applied. This approach was chosen deliberately, since its simplicity allows to precisely track the pathway of hydrogen and oxygen isotopes from their sources (for hydrogen CH_4, and for oxygen O_2 and O_3) to H_2O. The isotope fractionation factors of many reactions involved in the isotope transfer have not been measured up to now. Thus, the additional outcome of using a more sophisticated model is limited. As shown by Lyons (2001) and verified here (see Figs. 3, 9, and 10, and Table 5) a major unknown is the possible oxygen isotope exchange of O_2 with NO_x and HO_x. If the relevant reactions R34 and R35 are considered at their estimated upper limit, only a very weak mass-independent oxygen isotope signature is transferred to HO_x and H_2O.

Independent of the importance of reactions R34 and R35, the MIF signal transferred to HO_x (Fig. 1) and thus to H_2O as calculated by our model is only half as large as the one determined by Lyons (2001). This discrepancy arises from the different $\Delta^{17}O$ signatures assumed for the asymmetric O_3 molecule and $O(^1D)$. Lyons (2001) used the branching ratios of 0.43 and 0.57 measured for $\delta^{18}O$ in the reaction of $O + QO \longrightarrow OQO, QOO$ by (Janssen et al. (1999) also for $\delta^{17}O$, and the fractionation factors for this reaction measured by Mauersberger et al. (1999). This assumption led to $\Delta^{17}O$ values of asymmetric O_3 of $\Delta^{17}O(QOO) = \sim 85‰$, and together with the mean $\Delta^{17}O$ values of O_3 of $\Delta^{17}O(O_3) = \sim 38‰$, to $\Delta^{17}O$ values of symmetric O_3 of $\Delta^{17}O(OQO)) = -50‰$ (because $\Delta^{17}O(O_3) = 2/3\ \Delta^{17}O(QOO) + 1/3\ \Delta^{17}O(OQO))$. Such a strong $\delta^{17}O$ depletion of symmetric ozone is unlikely (C. Janssen, personal communication). In contrast, we assumed identical ratios of the enrichments of $\delta^{17}O$ and $\delta^{18}O$ in QOO and OQO. That is, in the stratosphere we assume mean $\Delta^{17}O$ values of 34‰ for O_3, which is in agreement with Lyons (2001), but $\Delta^{17}O$ values of 39‰ for QOO, and 25‰ for OQO.

7. Conclusions

A simple 1-D isotope chemistry box model is applied to derive vertical profiles of the stable isotope ratios D/H, $^{17}O/^{16}O$, and $^{18}O/^{16}O$ in middle atmospheric water vapour. It was demonstrated that a number of chemical reactions with diverse gases cause isotope fractionation in H_2O relative to values at the tropopause. This makes a description more complicated compared to other trace gases such as CO_2, CH_4, and N_2O.

$\delta D(H_2O)$ was modelled to increase from –660‰ at the tropopause to –430‰ above 40 km, which is in excellent agreement with the observations. This increase by ~230‰ corresponds to a fraction of ~40% of H_2O produced as end product of the oxidation of CH_4. Although the D fractionation factors of the individual CH_4 oxidation reactions with OH, $O(^1D)$, and Cl differ strongly, the $\delta D(H_2O)$ value tunrned out to be no sensitive

ACPD
3, 3991–4036, 2003

tracer to distinguish between the different CH_4 oxidation chains. This has two reasons. First, the major CH_4 loss occurs in the middle and upper stratosphere where the reactions with $O(^1D)$ dominate, accompanied by weak isotope fractionation dominates. Second, the chemical lifetime of H_2O is long in the middle atmosphere. This allows for significant mixing and thus weakening of the spatial gradients of $\delta D(H_2O)$.

The oxygen isotope ratios $\delta^{17}O(H_2O)$ and $\delta^{18}O(H_2O)$ are calculated to increase relative to the tropopause by up to ~85‰ and ~140‰, respectively, which is also in agreement with the observations. Fractionation of the oxygen isotope ratios in H_2O was demonstrated to be determined almost exclusively by the isotope signature of OH. The oxygen isotopic composition of OH, in turn, is mainly controlled by the one of mass-dependently fractionated O_2. Depending on the altitude and assumed reaction rates for isotope exchange reactions with O_2 (reactions R34 and R35) between 60 and almost 100% of all oxygen atoms transferred to H_2O stem from O_2, while 40 to 0% originate from O_3. The transfer of mass-independent fractionation in O_3 to OH and thus to H_2O in the stratosphere proceed primarily via NO_x species. In the mesosphere, however, it directly takes place via the reaction of $H + O_3 \rightarrow OH + O_2$. Maximum $\Delta^{17}O(H_2O)$ values of 10‰ around 35 km are calculated.

The largest unknowns in our calculations are the unquantified reaction rates of a few oxygen isotope exchange reactions, in particular of OH_x and NO_x with O_2, and the many unquantified isotope fractionation factors of the reactions involved in the isotope transfer to H_2O. In this respect, the most urgent need in this research field is the development of more precise techniques to measure the isotope composition of water vapour both in the laboratory and atmosphere.

Acknowledgements. We thank C. Brühl (MPI for Chemistry, Mainz) for his assistance in the provision of parameter profiles and U. Platt for his scientific assistance.

References

Anderson, S. M., Morton, J., and Mauersberger, K.: Laboratory measurements of ozone isotopomeres by tunable diode laser absorption spectroscopy, Chem. Phys. Lett., 156, 175–180, 1989.

Baertschi, P.: Absolute $^{18}0$ content of standard mean ocean water, Earth and Plan. Sci. Lett., 31, 341–344, 1976.

Barth, V. and Zahn, A.: Oxygen isotope composition of carbon dioxide in the middle atmosphere, J. Geophys. Res., 102, 12 995–10 007, 1997.

Brasseur, G. P. and Solomon, S.: Aeronomy of the middle atmosphere, D. Reidel Publishing Company, Dordrecht/Boston/Lancaster/Tokyo, 1986.

Cliff, S. S. and Thiemens, M. H.: The $^{18}O/^{16}O$ and $^{17}O/^{16}O$ ratios in atmospheric nitrous oxide: A mass-independent anomaly, Science, 278, 1774–1775, 1997.

Cliff, S. S., Brenninkmeijer, C. A. M., and Thiemens, M. H.: First measurement of the $^{18}O/^{16}O$ and $^{17}O/^{16}O$ ratios in stratospheric nitrous oxide: A mass-independent anomaly, J. Geophys. Res., 104, 16 171–16 175, 1999.

Coplen, T. B., Bohlke, J. K., De Bievre, P., Ding, T., Holden, N. E., Hopple, J. A., Krouse, H. R., Lamberty, A., Peiser, H. S., Revesz, K., Rieder, S. E., Rosman, K. J. R., Roth, E., Taylor, P. D. P., Vocke, R. D., Xiao, Y. K.: Isotope-abundance variations of selected elements (IUPAC Technical Report), Pure Appl. Chem., 74, 10, 1987–2017, 2002.

Craig, H.: Standard for reporting concentrations of deuterium and oxygen-18 in natural waters, Science, 133, 1833–1834, 1961.

Crutzen, P. J.: Methane's sinks and sources, Nature, 350, 380–381, 1991.

Crutzen, P. J.: On the role of CH_4 in atmospheric chemistry: sources, sinks and possible reductions in anthropogenic sources, Ambio, 24, 52–55, 1995.

DeMore, W. B., Howard, C. J., Sander, S. P., Ravishankara, A. R., Golden, D. M., Kolb, C. E., Hampson, R. F., Molina, M. J., and Kurylo, M. J.: Chemical kinetics and photochemical data for use in stratospheric modeling, Pasadena, CA: JPL Publication 97-4, 1997.

Dessler, A. E., Weinstock, E. M., Anderson, J. G., and Chan, K. R.: Mechanisms controlling water vapor in the lower stratosphere: A tale of two stratospheres, J. Geophys. Res., 100, 23 167–23 172, 1995.

DeWit J. C., Van der Straaten, C. M., and Mook, W. G.: Determination of the absolute D/H ratio of V-SMOW and SLAP, Geostand. Newslett., 4, 33–36, 1980.

Dinelli, B. M., Lepri, G., Carlotti, M., Carli, B., Mencaraglia, F., Ridolfi, M., Nolt, I. G., and Ade, P. A. R.: Measurements of the isotope ratio distribution of $HD^{16}O$ and $H_2^{18}O$ in the 20-38 km altitude range from far-infrared spectra, Geophys. Res. Lett., 24, 2003–2006, 1997.

Dinelli, B. M., Carli, B., and Carlotti, M.: Measurement of stratospheric distribution of $H_2^{16}O$, $H_2^{18}O$, $H_2^{17}O$ and $HD^{16}O$ from far infrared spectra, J. Geophys. Res., 96, 7509–7514, 1991.

Dubey, K., Mohrschladt, R., Donahue, N. M., and Anderson, J. G.: Isotope specific kinetics of hydroxyl radical (OH) with water (H_2O): Testing models of reactivity and atmospheric fractionation, J. Phys. Chem., 101, 1494–1500, 1997.

Forster, P. M. de F. and Shine, K. P.: Stratospheric water vapour changes as a possible contributor to observed stratospheric cooling, Geophys. Res. Lett., 26, 3309–3312, 1999.

Forster, P. M. de F. and Shine, K. P.: Assessing the climate impacts of trends in stratospheric water vapor, Geophys. Res. Lett., 29, 10.1029/2001GL013909, 2002.

Friedmann, I. and Scholz, T. G.: Isotopic composition of atmospheric hydrogen, 1967-1969, J. Geophys. Res., 79, 785–788, 1974.

Froidevaux, L. and Yung, Y. L.: Radiation and chemistry in the stratosphere: Sensitivity to O_2-absorption cross sections in the Herzberg continuum, Geophys. Res. Lett., 9, 854–857, 1982.

Gettelman, A., Holton, J. R., and Rosenlof, K. H.: Mass fluxes of O_3, CH_4, N_2O and CF_2Cl_2 in the lower stratosphere calculated from observational data, J. Geophys. Res., 102, 19 149–19 159, 1997.

Gierczak, T., Talukdar, R. K., Herdon, S., Vaghjiani, G. L., and Ravishankara, A. R.: Rate coefficients for the reactions of hydroxyl radicals with methane and deuterated methanes, J. Phys. Chem., 101, 3125–3134, 1997.

Greenblatt, G. D. and Howard, C. J.: Oxygen Atom Exchange in the Interaction of ^{18}O with Several Small Molecules, J. Phys. Chem., 93, 1035–1042, 1989.

Günther, J., Erbacher, B., Krankowsky, D., and Mauersberger, K.: Pressure dependence of two relative ozone formation rate coefficients, Chem. Phys. Lett., 306, 209–213, 1999

Guo, J., Abbas, M. M., and Nolt, I. G.: Stratospheric $H_2{}^{18}O$ distribution from infrared observations, Geophys. Res. Lett., 16, 1277–1280, 1989.

Hagemann, R., Nier, G., and Roth, E.: Absolute isotopic scale for deuterium analysis of natural waters. Absolute D/H ratio for SMOW, Tellus, 22, 712–715, 1970.

Holdsworth, G., Fogarasi, S., and Krouse, H. R.: Variation of stable isotopes of water with

altitude in the Saint Elias Mountains of Canada, J. Geophys. Res., 96, 7483–7494, 1991.
Holton, J. R., Haynes, P. H., McIntyre, M. E., Douglass, A. R., Rodd, R. B., and Pfister, L.: Stratosphere-troposphere exchange, Rev. Geophys., 33, 403–439, 1995.
Hurst, D. F., Dutton, G. S., Romashkin, P. A., Wamsley, P. R., Moor,e F. L., Elkins, J.W., Hintsa, E. J., Weinstock, E. M., Herman, R. L., Moyer, E.J., Scott, D.C., May, R. D., and Webster, C. R.: Closure of the total hydrogen budget of the northern extratropical lower stratosphere, J. Geophys. Res., 104, 8191–8200, 1999
IPCC, Climate Change 2001: The Scientific Basis, Contribution of Working Group I to the Third Assessment Report of the Intergovernmental Panel on Climate Change (IPCC) J.T. Houghton, Y. Ding, D.J. Griggs, M. Noguer, P.J. van der Linden, and D. Xiaosu (Eds.), Cambridge University Press, UK, pp. 944, 2001.
Janssen, C., Guenther, J., Krankowsky, D., and Mauersberger, K.: Relative formation rates of $^{50}O_3$, and $^{52}O_3$ in ^{16}O - ^{18}O mixtures, J. Chim. Phys., 111, 7179–7182, 1999.
Johnson, D. G., Jucks, K. W., Traub, W. A., and Chance, K. V.: Isotopic composition of stratospheric water vapor: Measurements and photochemistry, J. Geophys. Res., 106, 12 211–12 218, 2001a.
Johnson, D. G., Jucks, K. W., Traub, W. A., and Chance, K. V.: Isotopic composition of stratospheric water vapor: Implications for transport J. Geophys. Res., 106, 12 219–12 226, 2001b.
Kaiser, J., Brenninkmeijer, C. A. M., and Röckmann, T.: Intramolecular ^{15}N and ^{18}O fractionation in the reaction of N_2O with $O(^1D)$ and its implications for the stratospheric N_2O isotope signature, J. Geophys. Res., 107, 10.1029/2001JD001506, 2002.
Kaye, J. A. and Strobel, D. F.: Enhancement of heavy ozone in the Earth's atmosphere?, J. Geophys. Res., 88, 8447–8452, 1983
Kaye, J. A.: Analysis of the origins and implications of the ^{18}O content of stratospheric water vapour, J. Atmos. Chem., 10, 39–51, 1990.
Keith, D. W.: Stratospheric-tropospheric exchange: Inferences from the isotopic composition of water vapour, J. Geophys. Res., 105, 15 167–15 173, 2000.
Khalil, M. A. K., Khalil, M. A. K., Shearer, M. J., and Rasmussen, R. A.: Methane sinks and distribution, in Atmospheric Methane: Sources, Sinks, and Role in Global Change, edited by M.A.K. Khalil, NATO ASI Ser. I, Vol. 13, Springer-Verlag, New York, 1993.
Kirk-Davidoff, D. B., Hintsa, E. J., Anderson, J. G., and Keith, D. W.: The effect of climate change on ozone depletion through changes in stratospheric water vapour, Nature, 402,

399–401, 1999.
Kuang, Z., Toon, G. C., Wennberg, P. O., and Yung, Y. L.: Measured HDO/H_2O ratios across the tropical tropopause, Geophys. Res. Lett., 30(7) 1372, doi: 10.1029/2003GL017023, 2003.
Lary, D. J. and Toumi, T.: Halogen-catalyzed methane oxidation, J. Geophys. Res., 102, 23 421–23 428, 1997.
Lelieveld, J. and Crutzen, P. J.: Influences of cloud photochemical processes on tropospheric ozone, Nature, 343, 227–233, 1990.
Lelieveld, J. and Crutzen, P. J.: Role of deep convection in the ozone budget of the troposphere, Science, 264, 1759–1761, 1994.
Lelieveld, J., Crutzen, P. J., and Dentener, F. J.: Changing concentration, lifetime and climate forcing of atmospheric methane, Tellus, 50B, 128–150, 1998
Le Texier, H., Solomon, S., and Garcia, R. R.: The role of molecular hydrogen and methane oxidation in the water vapour budget of the stratosphere, Q.J.R. Meteorol. Soc., 114, 281–295, 1988.
Li, W., Baoling, N., Deqiu, J., and Qingliang, Z.: Measurement of the absolute abundance of oxygen-17 in VSMOW, Kexue Tongbao (Chinese Science Bulletin), 33, 1610–1613, 1988.
López-Valverde, M. A., López-Puertas, M., Remedios, J. J., Rodgers, C. D., Taylor, F. W., Zipf, E. C., and Erdman, P. W.: Validation of measurements of carbon monoxide from the improved stratospheric and mesospheric sounder, J. Geophys. Res., 101, 9929–9955, 1996.
Luz, B., Barkan, E., Bender, M. L., Thiemens, M.H., and Boering, K.A.: Triple-isotope composition of atmospheric oxygen as a tracer of biosphere productivity, Nature, 400, 547–550, 1999.
Lyons, J. R.: Transfer of mass-independent fractionation in ozone to other oxygen-containing radicals in the atmosphere, Geophys. Res. Lett., 28, 3231–3234, 2001.
Masgrau, L., González-Lafont, A., and Lluch, J. M.: Mechanism of the gas-phase HO + $H2_O \rightharpoonup H_2O$ + OH reaction and several associated isotope exchange reactions: A canonical variational transition state theory plus multidimensional tunneling calculation, J. Phys. Chem.A, 103, 1044–1053, 1999.
Massie S. T. and Hunten, D. M.: Stratospheric eddy diffusion coefficients from tracer data, J. Geophys. Res., 86, 9859–9868, 1981.
Mauersberger, K., Erbacher, B., Krankowsky, D., Günther, J., and Nickel, R.: Ozone isotope enrichment: Isotopomer-Specific rate coefficients, Science, 283, 370–372, 1999.
Mauersberger, K., Lämmerzahl, P., and Krankowsky, D.: Stratospheric ozone isotope enrich-

ments revisited, Geophys. Res. Lett., 28, 3155–3158, 2001.
Michelsen, H. A., Irion, F. W., Manney, G. L., Toon, G. C., and Gunson, M. R.: Features and trends in Atmospheric Trace Molecules Spectroscopy (ATMOS) version 3 stratospheric water vapor and methane measurements, J. Geophys. Res., 105, 11 713–22 724, 2000.
Morton, J., Barnes, J., Schueler, B., and Mauersberger, K.: Laboratory studies of heavy ozone, J. Geophys. Res., 95, 901–907, 1990
Moyer, E. J., Irion, F. W., Yung, Y. L., and Gunson, M. R.: ATMOS stratospheric deuterated water and implications for troposphere-stratosphere transport, Geophys. Res. Lett., 23, 2385–2388, 1996.
Oltmans, S. J. and Hofmann, D. J.: Increase in lower-stratospheric water vapour at a mid-latitude Northern Hemisphere site from 1981 to 1994, Nature, 374, 146–149, 1995.
Pollock, W., Heidt, L. E., Lueb, R., and Ehhalt, D. H.: Measurement of stratospheric water vapour by cryogenic collection, J. Geophys. Res., 85, 5555–5568, 1980.
Quay, P., Stutsman, J., Wilbur, D., Snover, A., Dlugokencky, E., and Brown, T.: The isotopic composition of atmospheric methane, Global Biogeochem. Cycles, 13, 445–461, 1999.
Randel, W. J., Wu, F., Gettelmann, A., Russell III, J. M., Zawodny, J. M., and Oltmans, S. J.: Seasonal variation of water vapor in the lower stratosphere observed in Halogen Occultation Experiment data, J. Geophys. Res., 106, 14 313–14 325, 2001.
Ridal, M., Jonsson, A., Werner, M., and Murtagh, D. P.: A one-dimensional simulation of the water vapor isotope HDO in the tropical stratosphere, J. Geophys. Res., 106, 32 283–32 294, 2001.
Ridal, M.: Isotopic ratios of water vapor and methane in the stratosphere: comparison between ATMOS measurements and a one-dimensional model, J. Geophys. Res., 107, 10.1029/2001JD000708, 2002.
Rinsland, C. P., Gunson, M. R., Foster, J. C., Toth, R. A., Farmer, C. B., and Zander, R.: Stratospheric profiles of heavy water vapour isotopes and CH_3D from analysis of the ATMOS Spacelab 3 infrared solar spectra, J. Geophys. Res., 96, 1057–1068, 1991.
Rinsland C. P., A. Goldman, V., Malathy Devi, B., Fridovich, D. G. S., Snyder, G .D., Jones, F .J., Murcray, D. G., Murcray, M. A. H., Smith, R. K., Seals, Jr., Coffey. M. T., and W. G. Mankin: Simultaneous stratospheric measurements of H_2O, HDO, CH_4 from balloon-borne and aircraft infrared solar absorption spectra and tunable diode laser spectroscopy of HDO, J. Geophys. Res., 89, 7259–7266, 1984.
Röckmann, T., Kaiser, J., Brenninkmeijer, C. A. M., Crowley, J. N., Borchers, R., Brand, W. A.,

and Crutzen, P. J.: Isotopic enrichment of nitrous oxide ($^{15}N^{14}NO$, $^{14}N^{15}NO$, $^{14}N^{14}N^{18}O$) in the stratosphere and in the laboratory, J. Geophys. Res., 106, 10 403–10 410, 2001.

Rozanski, K., Araguas-Araguas, L., Gonfiantini, R.: Isotopic patterns in modern global precipitation, Climate change in continental isotopic records, Geophys. Monograph, 78, 1–36, 1993.

Rosenlof, K. H., Tuck, A. F., Kelly, K. K., Russell III, J. M.: and McCormick, M. P.: Hemispheric asymmetries in water vapour and inferences about transport in the lower stratosphere, JGR, 102, 13 213–13 234, 1997.

Rosenlof, K. H., Oltmans, S. J., Kley, D., Russell, J. M., Chiou, E. W., Chu, W. P., Johnson, D. G., Kelly, K. K., Michelsen, H. A., Nedoluha, G. E., Remsberg, E. E., Toon, G. C., and McCormick, M. P.,: Stratospheric water vapor increases over the past half-century, Geophys. Res. Lett., 1195–1198, 2001.

Rosenlof, K. H.: Transport changes inferred from HALOE water and methane measurements, J. Meteorol. Soc. Jpn., 80, 4B, 831–848, 2002.

Saueressig G., Bergamaschi, P., Crowley, J. N., and Fischer, H.: D/H kinetic isotope effect in the reaction CH_4 + Cl, Geophys. Res. Lett., 23, 3619–3622, 1996.

Saueressig G., Crowley, J. N., Bergamaschi P., Brühl, C., Brenninkmeijer, C. A. M., and Fischer, H.: Carbon 13 and D kinetic isotope effects in the reactions of CH_4 with $O(^1D)$ and OH: New laboratory measurements and their implications for the isotopic composition of stratospheric methane, J. Geophys. Res., 106, 23 127–23 138, 2001.

Sharma, H. D., Jervis, R. E., and Wong, K. Y.: Isotopic exchange reactions in nitrogen oxides, J. Phys. Chem., 74, 923–933, 1970.

Smith, R. B.: Deuterium in North Atlantic storm tops, J. Atmos. Sci., 49, 2041–2057, 1992.

SPARC, SPARC assessment of upper tropospheric and stratospheric water vapour, ed. D. Kley, J.M. Russell III, and C. Phillips, SPARC report No. 2, 2000.

Stowasser, M., Oelhaf, H., Wetzel, G., Friedl-Vallon, F., Maucher, G., Seefeldner, M., Trieschmann, O., Clarmann, T. V.: Simultaneous measurements of HDO, H_2O, and CH_4 with MIPAS-B: Hydrogen budget and indication of dehydration inside the polar vortex, J. Geophys. Res., 104, 19 213–19 225, 1999.

Taylor, C. B.: Vertical distribution of deuterium in atmospheric water vapour: problems in application to assess atmospheric condensation models, Tellus, 36B, 67–72, 1984.

Thiemens, M. H. and Heidenreich III, J. E.: The mass-independent fractionation of oxygen: A novel isotope effect and its possible cosmochemical implications, Science, 219, 1073–1075,

1983.
Thiemens, M. H. and Jackson, T.: New experimental evidence for the mechanism for production of isotopically heavy ozone, Geophys. Res. Lett., 15, 639–642, 1988.
Thiemens, M. H. and Jackson, T.: Pressure dependency for heavy isotope enhancement in ozone formation, Geophys. Res. Lett., 17, 717–719, 1990.
Tse, R. S., Wong, S. C., and Yuen, C. P.: Determination of deuterium/hydrogen ratios in natural waters by Fourier transform nuclear magnetic resonance spectrometry, Anal. Chem., 52, 2445–2447, 1980.
Tyler, S. C., Ajie, H. O., Rice, A. L., Cicerone, R. J., and Tuazon, E. C.: Experimentally determined kinetic isotope effects in the reaction of CH_4 with Cl: Implications for atmospheric CH_4, Geophys. Res. Lett., 27, 1715–1718, 2000.
Webster, C. R.: In situ measurements of HDO, $H_2{}^{16}O$, $H_2{}^{18}O$, and $H_2{}^{17}O$ in the upper troposphere and lower stratosphere using tunable laser absorption spectroscopy, Geophysical Research Abstracts, Vol. 5, 12861, European Geophysical Society (EGS), XXVIII General Assembly, Nice, France, 6–11 April, 2003.
Wen, J. and Thiemens, M. H.: Multi-isotope study of the $O(^1D)$ + CO_2 exchange and stratospheric consequences, J. Geophys. Res., 98, 12 801–12 808, 1993.
Yang, H. and Tung, K. K.: Cross-isentropic stratosphere-troposphere exchange of mass and water vapour, J. Geophys. Res., 101, 9413–9423, 1996.
Yung, Y. L., DeMore, W. B., and Pinto, J. P.: Isotope exchange between carbon dioxide and ozone via $O(^1D)$ in the stratosphere, Geophys. Res. Lett., 18, 13–16, 1991.
Yung, Y. L., Lee, A. Y. T., Irion, F. W., DeMore, W. B., and Wen, J.: Carbon dioxide in the atmosphere: Isotopic exchange with ozone and its use as tracer in the middle atmosphere, J. Geophys. Res., 102, 10 857–10 866, 1997.
Zahn, A.: Constraints on 2-way transport across the Arctic tropopause based on O_3, stratospheric tracer (SF_6) ages, and water vapor isotope (D, T) tracers, J. Atmos. Chem., 39, 303–325, 2001.
Zahn, A., Barth, V., Pfeilsticker, K., and Platt, U.: Deuterium, Oxygen-18 and tritium as tracers for water vapour transport in the lower stratosphere and tropopause region, J. Atmos. Chem., 30, 25–47, 1998.
Zöger, M., Engel, A., McKenna, D. S., Schiller, C., Schmidt, U., and Woyke, T.: Balloon-borne in situ measurements of stratospheric H_2O, CH_4 and H_2 in midlatitudes, J. Geophys. Res., 104, 1817–1825, 1999.

Table 1. Considered gas phase reactions

No	reaction	Rate A	Rate E	Ref. [a]
1	$CH_4 + OH \longrightarrow H_2O + CH_3$	Table 3		
2	$CH_4 + O(^1D) \longrightarrow OH + CH_3$	Table 3		
3	$CH_4 + Cl \longrightarrow HCl + CH_3$	Table 3		
4	$CH_4 + \gamma \longrightarrow H + CH_3$	Table 3		
5	$CH_3O + O_2 \longrightarrow HO_2 + H_2CO$	3.9(-14)	900	JPL97
6	$CH_3 + O_2 + M \longrightarrow CH_3O_2 + M$	Table 2		
7	$CH_2O + OH \longrightarrow H_2O + HCO$	1.0(-11)	0	JPL97
8	$CH_2O + \gamma \longrightarrow H + HCO/H_2 + CO$	altitude dependent		
9	$CH_2O + O(^3P) \longrightarrow OH + HCO$	3.4(-10)	1600	JPL97
10	$CH_2O + Cl \longrightarrow HCl + HCO$	8.1(-11)	30	JPL97
11	$HCO + O_2 \longrightarrow HO_2 + CO$	3.5(-12)	-140	JPL97
12	$H + O_2 + M \longrightarrow HO_2 + M$	Table 2		
13	$H + O_3 \longrightarrow OH + O_2$	1.4(-10)	470	JPL97
14	$H + HO_2 \longrightarrow H_2O + O(^3P)$	3.7(-11)	2300	JPL97
15	$OH + HO_2 \longrightarrow H_2O + O_2$	4.8(-11)	-250	JPL97
16	$OH + O_3 \longrightarrow HO_2 + O_2$	1.6(-12)	940	JPL97
17	$OH + O(^3P) \longrightarrow H + O_2$	2.2(-11)	-120	JPL97
18	$OH + OH \longrightarrow H_2O + O(^3P)$	4.2(-12)	240	JPL97
19	$OH + NO_2 + M \longrightarrow HNO_3 + M$	Table 2		
20	$HCl + OH \longrightarrow H_2O + Cl$	2.6(-12)	350	JPL97
21	$CO + OH \longrightarrow CO_2 + H$	1.5(-13)	0	JPL97
22	$HO_2 + NO \longrightarrow OH + NO_2$	3.5(-12)	-250	JPL97
23	$HO_2 + O(^3P) \longrightarrow OH + O_2$	3.0(-11)	-200	JPL97
24	$HO_2 + O_3 \longrightarrow OH + 2 \cdot O_2$	1.1(-14)	500	JPL97

ACPD
3, 3991–4036, 2003

Table 1. Continued

No	reaction	Rate A	Rate E	Ref. [a]
25	$H_2 + OH \longrightarrow H_2O + H$	5.5(-12)	2000	JPL97
26	$H_2 + O(^1D) \longrightarrow H + OH$	1.1(-10)	0	JPL97
27	$H_2 + Cl \longrightarrow H + HCl$	3.7(-11)	2300	JPL97
28	$HNO_3 + OH \longrightarrow H_2O + NO_3$			JPL97
29	$H_2O + O(^1D) \longrightarrow 2 \cdot OH$	2.2(-10)	0	JPL97
30	$H_2O + \gamma \longrightarrow H + OH$	5(-6)	-4.4(-19)	n=0.917; BS [b]

[a] JPL97: DeMoore et al. (1997), BS: Brasseur and Solomon (1986)
[b] photolysis rate $j(z) = A \cdot \exp[E \cdot L(z)^n]$ in s^{-1}, L(z) being the number of molecules per cm^2 above altitude z.

ACPD
3, 3991–4036, 2003

Table 2. Termolecular reactions

No.	Reaction	k_0^{300} [a]	N	k_∞^{300} [b]	m	Reference
6	$CH_3 + O_2 + M \longrightarrow CH_3O_2 + M$	$4.5 \cdot 10^{-31}$	3.0	$1.8 \cdot 10^{-12}$	1.7	JPL97
12	$H + O_2 + M \longrightarrow HO_2 + M$	$5.7 \cdot 10^{-32}$	1.6	$7.5 \cdot 10^{-11}$	0.0	JPL97
19	$OH + NO_2 + M \longrightarrow HNO_3 + M$	$2.5 \cdot 10^{-30}$	4.4	$1.6 \cdot 10^{-11}$	1.7	JPL97

[a] $k_0(T) = k_0^{300} \cdot (\frac{T}{300})^{-n}$
[b] $k_\infty(T) = k_\infty^{300} \cdot (\frac{T}{300})^{-m}$
rate constant $k(M,T) = (\frac{k_0(t)[M]}{1+(k_0(T)[M]/k_\infty(T))}) \cdot 0.6^{(1+[log_{10}(k_0(t)[M]/k_\infty(T))]^2)^{-1}}$
$[M]$ being the number concentrations of air molecules and T the temperature.

ACPD
3, 3991–4036, 2003

Table 3. Detailed description of the initial methane destruction reactions

No	reaction	rate A	rate E	branching ratio	fractionation factor	Ref. [a]
1	$CH_4 + OH \longrightarrow H_2O + CH_3$	2.45 (−12)	1775	1	1	JPL97
	$CH_4 + {}^{17}OH \longrightarrow H_2{}^{17}O + CH_3$	2.45 (−12)	1775	1	0.986	JPL97
	$CH_4 + {}^{18}OH \longrightarrow H_2{}^{18}O + CH_3$	2.45 (−12)	1775	1	0.973	JPL97
	$CH_4 + OD \longrightarrow HDO + CH_3$	2.45 (−12)	1775	1	0.986	JPL97
	$CH_3D + OH \longrightarrow H_2O + CDH_2$	2.45 (−12)	1775	0.75	1	JPL97
	$CH_3D + OH \longrightarrow HDO + CH_3$	3.5 (−12)	1950	0.25	1	JPL97
	$CH_3D + OD \longrightarrow D_2O + CH_3$	3.5 (−12)	1950	0.25	0.986	JPL97
	$CH_3D + OD \longrightarrow HDO + CH_2D$	3.5 (−12)	1950	0.75	0.986	JPL97
2	$CH_4 + O(^1D) \longrightarrow OH + CH_3$	1.5 (−10)	0	0.9	1	JPL97
	$CH_4 + {}^{17}O(^1D) \longrightarrow {}^{17}OH + CH_3$	1.5 (−10)	0	0.9	0.985	JPL97
	$CH_4 + {}^{18}O(^1D) \longrightarrow {}^{18}OH + CH_3$	1.5 (−10)	0	0.9	0.972	JPL97
	$CH_4 + O(^1D) \longrightarrow H_2CO + H_2$	1.5 (−10)	0	0.1	1	JPL97
	$CH_4 + {}^{17}O(^1D) \longrightarrow H_2C{}^{17}O + H_2$	1.5 (−10)	0	0.1	0.985	JPL97
	$CH_4 + {}^{18}O(^1D) \longrightarrow H_2C{}^{18}O + H_2$	1.5 (−10)	0	0.1	0.972	JPL97
	$CH_3D + O(^1D) \longrightarrow OD + CH_3$	1.5 (−10)	0	0.25 · 0.9	-0.037 · exp(0.224/T)	SE01
	$CH_3D + O(^1D) \longrightarrow OH + CH_2D$	1.5 (−10)	0	0.75 · 0.9	-0.037 · exp(0.224/T)	SE01
	$CH_3D + O(^1D) \longrightarrow H_2 + HDCO$	1.5 (−10)	0	0.5 · 0.1	-0.037 · exp(0.224/T)	SE01
	$CH_3D + O(^1D) \longrightarrow HD + H_2CO$	1.5 (−10)	0	0.5 · 0.1	-0.037 · exp(0.224/T)	SE01
3	$CH_4 + Cl \longrightarrow CH_3 + HCl$	1.1 (−11)	1400	1	1	JPL97
	$CH_3D + Cl \longrightarrow CH_3 + DCl$	1.1 (−11)	1400	0.25	1.278 · exp(51.31/T)	SE96
	$CH_3D + Cl \longrightarrow CH_2D + HCl$	1.1 (−11)	1400	0.75	1.278 · exp(51.31/T)	SE96
4	$CH_4 + \gamma \longrightarrow CH_3 + H$	5 (−6)	-4.4(-19)	1	n=0.917	BS [b]
	$CH_3D + \gamma \longrightarrow CH_3 + D$	5 (−6)	-4.4(-19)	0.25	n=0.917	BS
	$CH_3D + \gamma \longrightarrow CH_2D + H$	5 (−6)	-4.4(-19)	0.75	n=0.917	BS

[a] JPL97: DeMoore et al. (1997), BS: Brasseur and Solomon (1986), SE96: Saueressig et al. (1996), SE01: Saueressig et al. (2001).
[b] photolysis rate $j(z) = A \cdot \exp[E \cdot L(z)^n]$ in s^{-1}, L(z) being the number of molecules per cm^2 above altitude z.
rate constant $k(T) = A \cdot \exp[-(E \cdot [K]/T)]$ in $cm^3 s^{-1}$

ACPD
3, 3991–4036, 2003

Table 4. Considered oxygen isotope exchange reactions

No	reaction	Rate A	Rate E	Ref.
31	$QH + NO \leftrightarrow OH + NQ$	1.8(-11)	0	Dubey et al. [1997]
32	$QH + NO_2 \leftrightarrow OH + NOQ$	1.0(-11)	0	Greenblatt and Howard [1989]
33	$QH + H_2O \leftrightarrow OH + H_2Q$	1.6(-13)	2100	Greenblatt and Howard [1989]
34	$QH + O_2 \leftrightarrow OH + OQ$	< 1(-17)	0	Greenblatt and Howard [1989]
35	$HOQ + O_2 \leftrightarrow HO_2 + OQ$	< 3(-17)	0	Sinha et al. [1987]
36	$NOQ + O_2 \leftrightarrow NO_2 + OQ$	< 1(-24)	0	Sharma et al. [1970]
37	$Q + O_2 \leftrightarrow OQ + O$			see Sect. 4.5
38	$Q + NO \leftrightarrow O + NQ$			see Sect. 4.5

ACPD
3, 3991–4036, 2003

Table 5. Percentage origin of oxygen isotopes of freshly produced H_2O averaged over stratosphere and mesosphere

Oxygen Isotope Source		neglecting R33, R34		considering R33, R34	
Species	isotope signature	stratosphere	mesosphere	stratosphere	mesosphere
O_2	MDF[a]	78.0	70.2	98.1	72.5
O_3	MIF[b]	17.4	29.8	1.9	27.5
$O(^1D)$	MIF[b]	2.3	0	0	0
others		2.3	0	0	0

[a] MDF = mass-dependently fractionated
[b] MIF = mass-independently fractionated

ACPD
3, 3991–4036, 2003

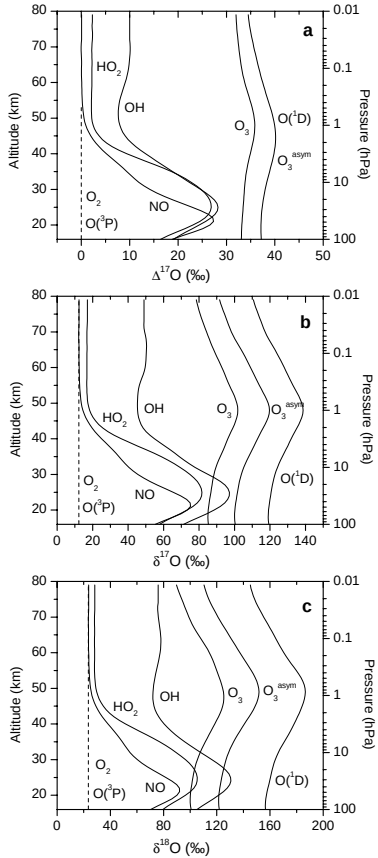

Fig. 1. Vertical profile of $\Delta^{17}O$ (graph a), $\delta^{17}O$ (graph b), and $\delta^{18}O$ (graph c) assumed for O_2, $O(^3P)$, O_3, asymmetric O_3, and $O(^1D)$, and calculated for NO, OH and HO_2 (without considering the isotope exchange reactions R34 and R35).

ACPD
3, 3991–4036, 2003

Isotope composition of middle atmospheric H_2O

Ch. Bechtel and A. Zahn

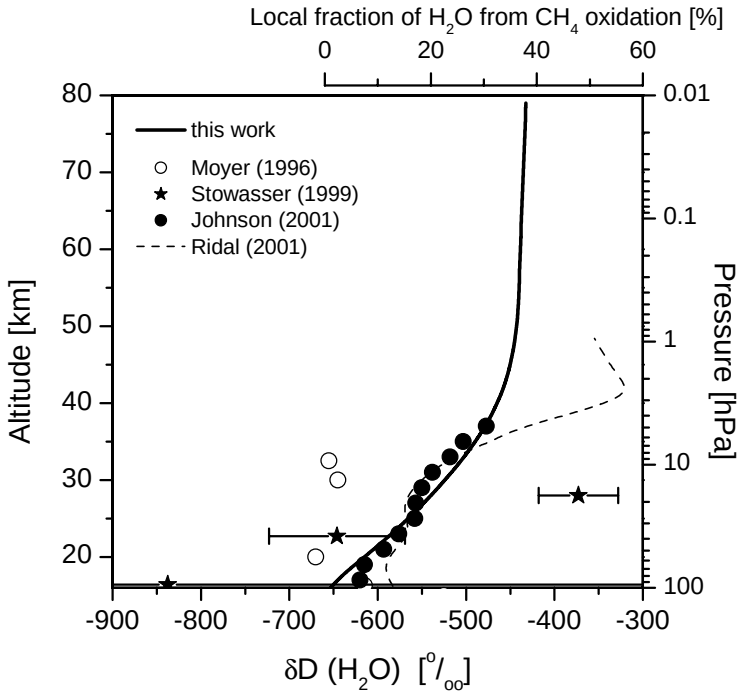

Fig. 2. Calculated vertical profile of $\delta D(H_2O)$ (solid line) compared to measurements. Open circles: ATMOS FTIR data of near-global latitudinal coverage (Moyer et al., 1996). Full circles: Smithsonian Astrophysical Observatory's far-infrared data by Johnson et al. [2001a]. Stars: Balloon-borne FTIR data inside the Arctic vortex at 68°N (Stowasser et al., 1999). Dashed line: 1-D model result by Ridal et al. (2001). Upper *x* axis indicates the approximate fraction of H_2O from the CH_4 oxidation inferred from the $\delta D(H_2O)$ value (explanation, see Sect. 6.2).

ACPD
3, 3991–4036, 2003

Isotope composition of middle atmospheric H_2O

Ch. Bechtel and A. Zahn

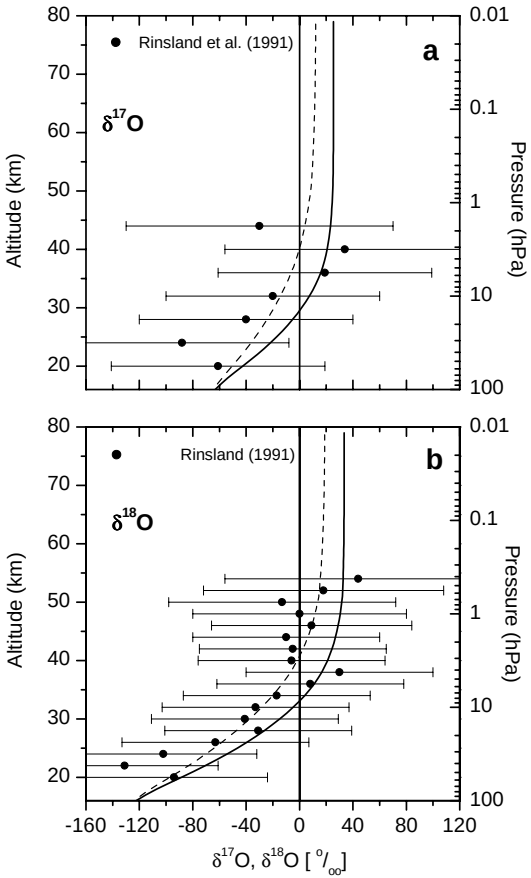

Fig. 3. Calculated vertical profiles of $\delta^{17}O(H_2O)$ (graph a) and $\delta^{18}O(H_2O)$ (graph b) compared to ATMOS Spacelab 3 infrared solar spectra near 30°N [Rinsland et al., 1991]. Straight lines: not quantified oxygen exchange reactions R34 and R35 are omitted. Dashed line: Those reactions are considered at their estimated upper limit.

ACPD
3, 3991–4036, 2003

Isotope composition of middle atmospheric H_2O

Ch. Bechtel and A. Zahn

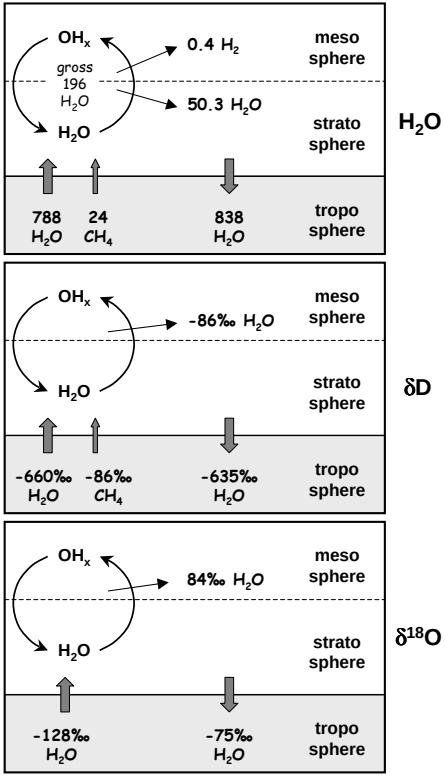

Fig. 4. Middle atmospheric budgets of **a**: H_2O, numbers are mass fluxes in Mt yr^{-1} (the flux into the stratosphere is adopted from Yang and Tung [1996], other numbers are model results), **b**: δD, numbers are mean δD values in ‰ of the individual species, and **c**: δ^{18}O, numbers are mean δ^{18}O values in ‰.

ACPD
3, 3991–4036, 2003

Isotope composition of middle atmospheric H_2O

Ch. Bechtel and A. Zahn

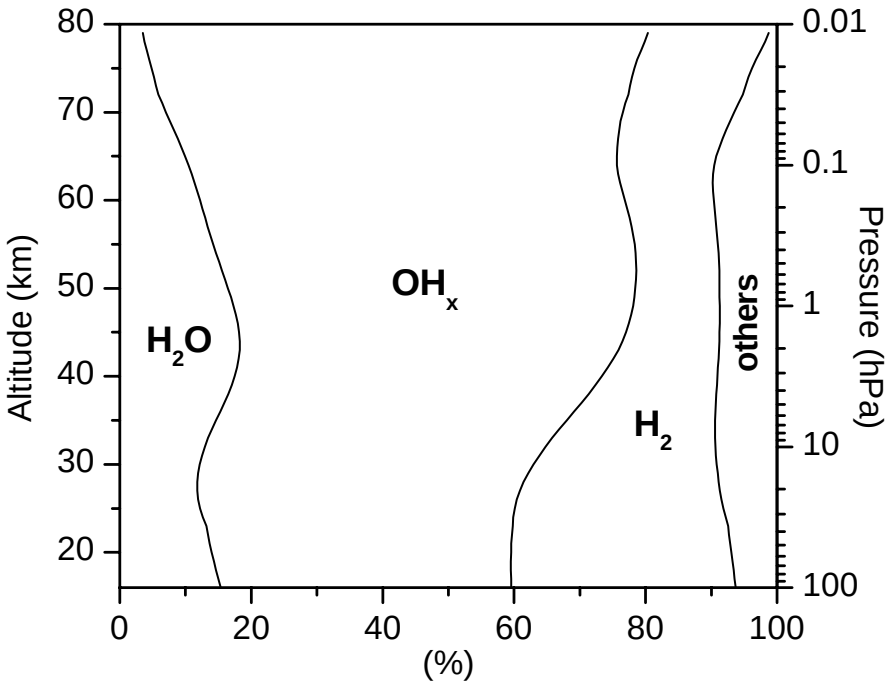

Fig. 5. Calculated percentage fraction of hydrogen atoms that are transferred during the initial oxidation reaction of CH_4 either to H_2O, OH_x, H_2, or other species (such as HCl).

ACPD
3, 3991–4036, 2003

Isotope composition of middle atmospheric H_2O

Ch. Bechtel and A. Zahn

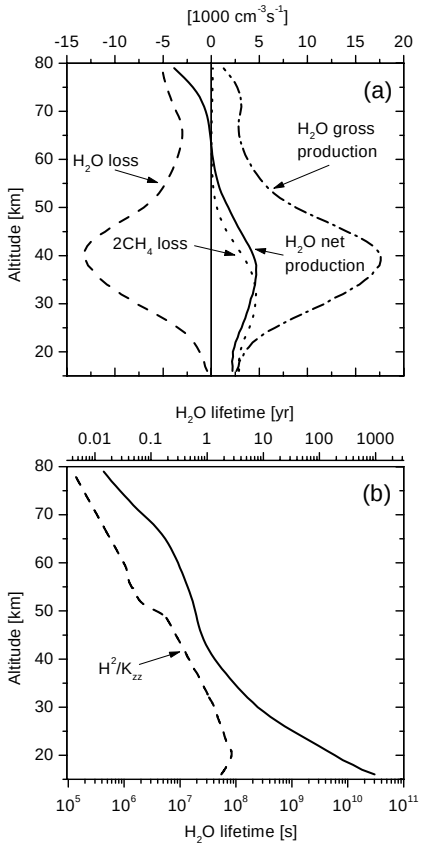

Fig. 6. **(a)** calculated vertical profiles of H_2O production and loss rates in the middle atmosphere. For comparison, the double CH_4 loss rate is shown (as almost two H_2O molecules are net produced for each oxidised CH_4 molecule, see Eq. 1). **(b)** comparison of the photochemical lifetime of water vapour (straight line) with the transport time scale (dashed line).

ACPD
3, 3991–4036, 2003

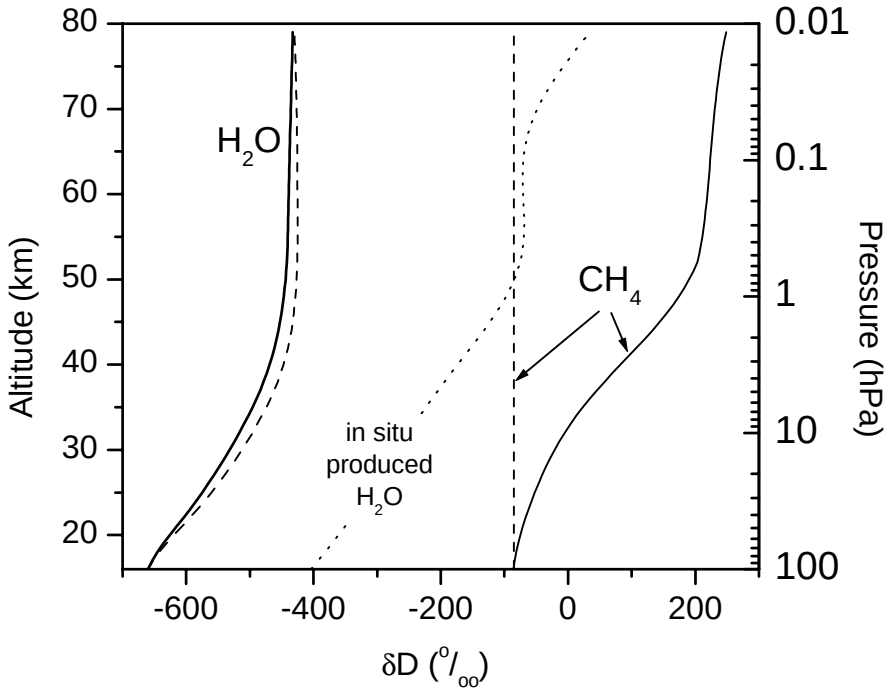

Fig. 7. Vertical profiles of $\delta D(CH_4)$ and $\delta D(H_2O)$. Solid lines: Fractionation during the methane decomposition reactions with OH, Cl, and $O(^1D)$ is allowed. Dashed lines: Fractionation is prevented. Dotted line: Isotope enrichment of freshly produced H_2O (while fractionation is allowed).

ACPD
3, 3991–4036, 2003

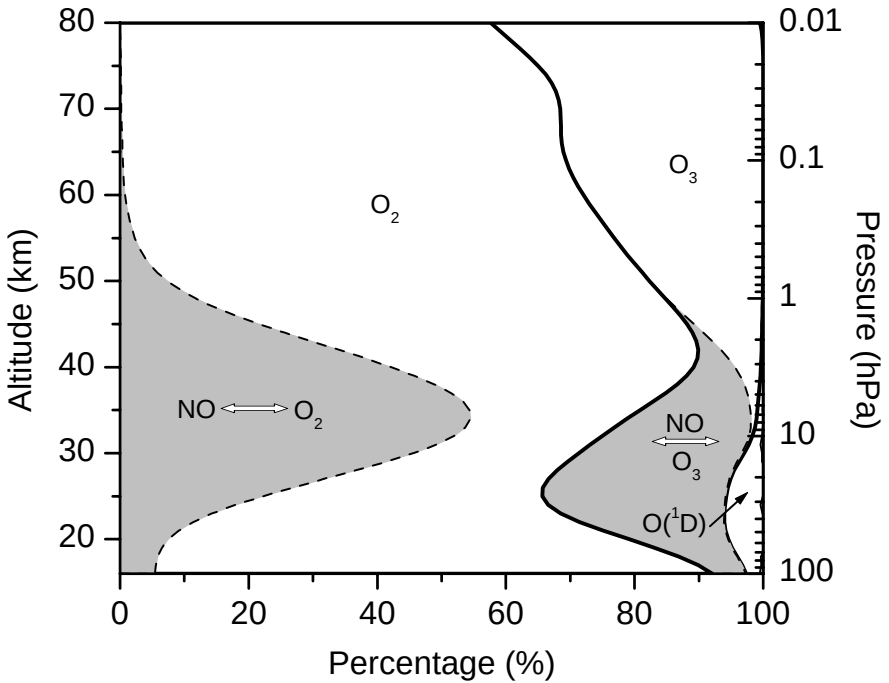

Fig. 8. Percentage fraction of oxygen atoms originating from the "reservoirs" O_2, O_3, and $O(^1D)$ in freshly produced H_2O. Thick straight lines separate the three different reservoirs. In the stratosphere, considerable oxygen transfer from O_2 and O_3 to H_2O occurs via the NO_x family (grey areas).

ACPD
3, 3991–4036, 2003

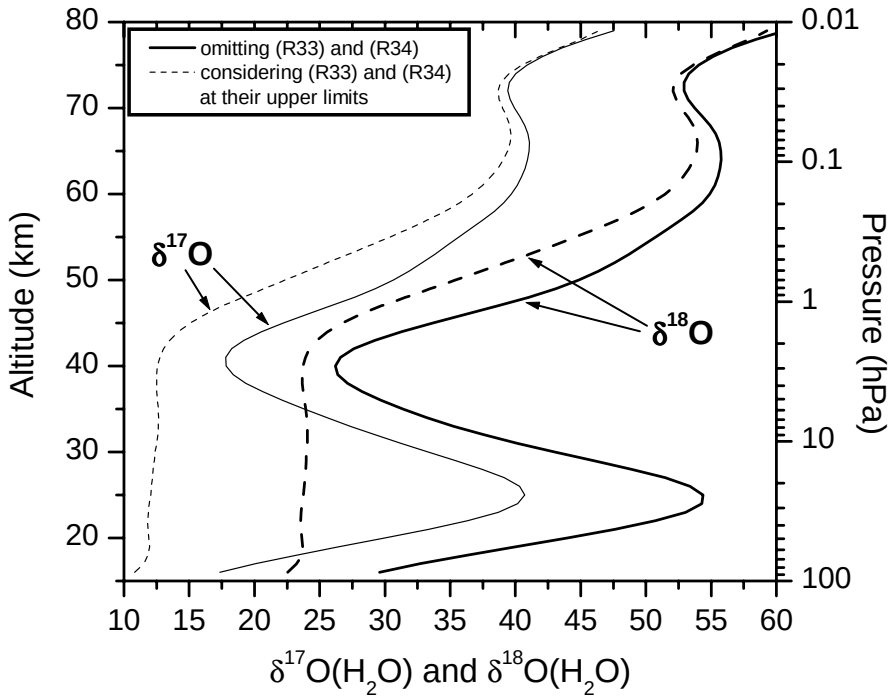

Fig. 9. Vertical profiles of $\delta^{17}O(H_2O)$ (thin lines) and $\delta^{18}O(H_2O)$ (thick lines) of freshly produced H_2O. Straight lines: additional oxygen exchange reactions R34 and R35 are neglected. Dashed lines: reactions R34 and R35 are considered using rate constants at their estimated upper limit.

ACPD
3, 3991–4036, 2003

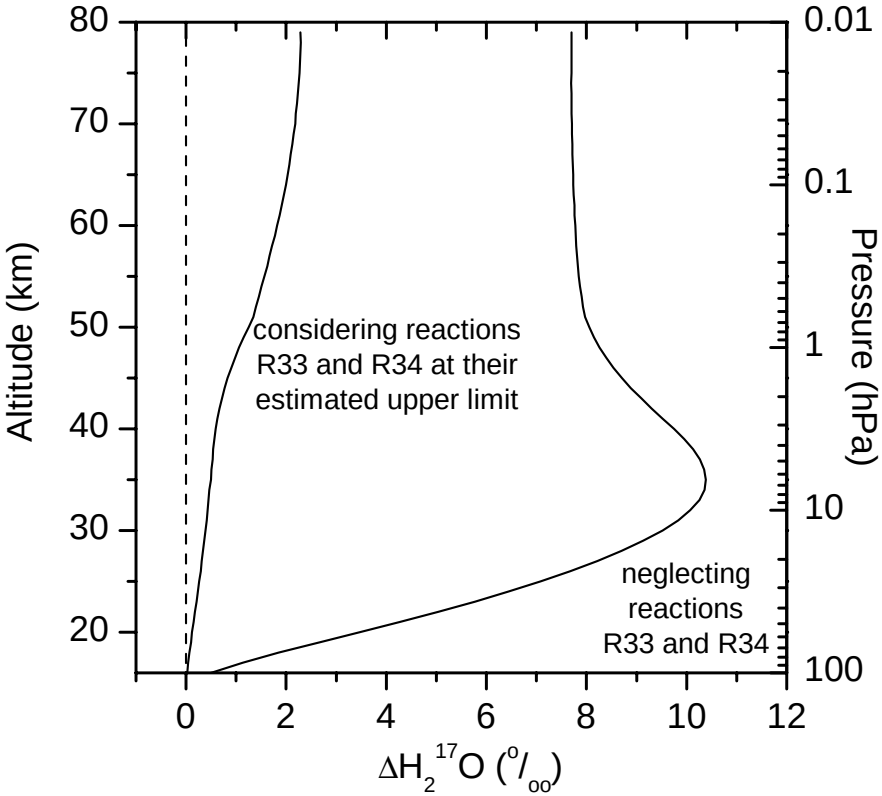

Fig. 10. Calculated vertical profile of $\Delta^{17}O(H_2O)$ when considering and neglecting the additional oxygen exchange reactions R34 and R35 at their estimated upper limit.

ACPD
3, 3991–4036, 2003